Pediatr Radiol (2013) 43:173–188
DOI 10.1007/s00247-012-2486-z

MINISYMPOSIUM

Cerebral sinovenous thrombosis in pediatric practice

Gary L. Hedlund

Received: 3 May 2012 / Revised: 9 July 2012 / Accepted: 26 July 2012 / Published online: 1 December 2012

Abstract Cerebral sinovenous thrombosis (CSVT) in the pediatric population is a relatively uncommon yet underappreciated and potentially life-threatening neurological condition. Early symptoms and signs are often vague and the clinician requesting a cranial imaging study might not even suspect sinovenous thrombosis. If left undiagnosed, or if the diagnosis of CSVT is delayed, progressive neurological deterioration, coma and death can follow. The purpose of this review is to highlight pertinent development of the cerebral venous system, discuss the causal factors of cerebral sinovenous thrombosis in the pediatric population, review practical imaging strategies using cranial sonography augmented with color and pulsed Doppler, unenhanced brain CT, CT venography, cerebral MRI, and MR venography (MRV). Finally, this review will illustrate the imaging features of sinovenous thrombosis, including a discussion of the common causes of false-positive and false-negative CT and MRI studies.

Keywords Cerebral sinovenous thrombosis · CT venography · 2-D time-of-flight · MR venography · 3-D SPGR · Children

Introduction

A variety of terms appears in the literature describing thrombus within intracranial venous structures. These terms include cerebral sinovenous thrombosis, dural sinus thrombosis, sinovenous thrombosis, deep cerebral venous thrombosis, cerebral vein thrombosis, intracranial venous thrombosis and cavernous sinus thrombosis.

Traditionally, intracranial venous thrombosis describes thrombus in at least one of three compartments. The superficial venous system (e.g., cortical dural veins, vein of Labbe, vein of Trolard), deep venous structures (e.g., internal cerebral veins, basal vein of Rosenthal, Great cerebral vein or vein of Galen) and the dural venous sinuses (enclosed in the leaves of the dura and representative of the major drainage pathways of the cerebral veins, e.g., superior sagittal, transverse and sigmoid venous sinuses) [1, 2]. In this review, the term cerebral sinovenous thrombosis (CSVT) is used to describe thrombus within one or more of these compartments.

The newborn, infant, child or adolescent afflicted with cerebral sinovenous thrombosis may present with a variety of symptoms and signs, including irritability, headache, seizure, encephalopathy, papilledema, cranial nerve palsies, motor weakness and coma. Additionally, the location of the thrombus and whether it is partial or complete, acute or chronic influences the clinical presentation. Across all pediatric age groups, seizures remain the most common presentation of CSVT. Seizures and coma at presentation represent poor clinical prognosticators [3–6]. Apart from seizures, irritability and hypotonia are observed more commonly among neonates and headache and motor symptoms predominate in the non-neonatal patients. Sinovenous thrombosis might be associated with serious neurological impairment, lifelong morbidity, and mortality in a minority of patients. Hemorrhagic infarctions (40%) and hydrocephalus (10%) represent important contributors to morbidity [7–9].

DeVeber et al. [10] in the Canadian cerebral venous thrombosis registry reported CSVT as a relatively rare event in pediatric patients, occurring with an estimated incidence of less than 1 per 100,000 between term birth and 18 years of age. These authors estimate that CSVT is the cause of approximately 20% of ischemic cerebral vascular disease in

G. L. Hedlund (✉)
Department of Medical Imaging, Primary Children's Medical Center, University of Utah School of Medicine,
100 N. Mario Capecchi Drive,
Salt Lake City, UT 84113, USA
e-mail: gary.hedlund@imail.org

children [10]. Neonates and infants in the first 6 months of life contribute significantly to the total number of documented cases of pediatric CSVT. The incidence of neonatal venous sinus thrombosis is estimated at 40.7 per 100,000 live births per year [3–7]. Carvalho et al. [3] reported that among 31 children with SVT, 61% were neonates. Other authors have reported a similar high proportion of neonates and young infants in their pediatric cohorts afflicted with CSVT [8]. In a multicenter study of pediatric cerebral venous sinus thrombosis, Wasay et al. [7] reported a mortality rate of 25% among neonates with CSVT.

The anatomical location and extent of sinovenous thrombosis varies based upon the etiology of the clot. In the multicenter study by Wasay et al. [7] the transverse sinus (73%) was more commonly involved, followed by the superior sagittal sinus (35%), and multiple anatomical sites of thrombosis were common (70%). Contiguous involvement of transverse and sigmoid venous sinuses might be as high as 90% [1, 7].

Cerebral venous development

A working understanding of cerebral venous development and common anatomical variations provides insight to the radiologist responsible for interpreting pediatric cranial imaging studies. Furthermore, in the setting of partial or complete cerebral sinovenous thrombosis, appreciation of collateral pathways of venous drainage allows the imaging physician to make critical observations that have important diagnostic, treatment and outcome impact.

In the final stages of cerebral venous development during the 3rd month of fetal life, much of the definitive venous system is established. In contrast to other areas of the body, the cerebral venous system shows much more morphological variability than the arterial system. Throughout fetal and early postnatal development, the venous system is continuously remodeling in a process of integrative development as a result of morphological changes occurring in the skull base and cerebral vesicles [11].

The main components of the cerebral venous system are the dural venous sinuses and the cerebral veins. The dural venous sinuses represent venous conduits invested by dura receiving blood from superficial and deep sources (Fig. 1). The cerebral veins can be further subdivided into superficial veins that drain the cortical and subcortical regions, and deep cerebral veins (medullary and subependymal) that drain blood from the periventricular white matter and basal ganglia (Fig. 1) [11].

Transcerebral veins connect the surface venous network with the subependymal veins. These transcerebral veins play a role in cerebrospinal fluid (CSF) resorption and cerebral nutrition. Dilation of these veins can be observed in states of augmented venous flow (e.g., arteriovenous malformation [AVM]), obstructed venous drainage (e.g., thrombosis), and elevated cerebral venous pressure [12]. Transcerebral veins that have only previously been observed in the venous phase of cerebral angiography have more recently been rendered visible by susceptibility-weighted MRI (SWI) (Fig. 1) [12, 13].

Recognizing common anatomical variations in dural venous sinus anatomy becomes particularly important in the clinical setting of dural venous sinus thrombosis. Developmentally, the superior sagittal sinus drains preferentially to the right transverse venous sinus and jugular vein. The straight sinus, which develops as the primary venous outflow of the deep venous system (choroid plexi of the lateral and third ventricles), drains preferentially to the left transverse sinus and jugular vein. These two venous systems typically unite at the torcular Herophili but in a small percentage of patients they are separate. Venous thrombosis of one venous limb could lead to inadequate venous drainage and serious clinical consequences [11]. The persistence of the falcine venous sinus is an important embryological venous system observed in the setting of vein of Galen malformation and atretic parietal cephalocele. In the latter condition, a lack of recognition that the palpable subcutaneous vertex mass is in fibrovascular continuity with the underlying dura, bifid superior sagittal venous sinus and falcine venous sinus could lead to unexpected hemorrhage or thrombosis during surgery (Fig. 1) [11].

Causal factors and pathophysiology

Some causal factors for the development of sinovenous thrombosis differ between the pediatric population and adults. The predisposing factors for CSVT can be broadly broken down into conditions that cause mechanical compression of the vein or venous sinus with resultant venous stasis and occlusion, and invasion of the vessel or dural venous sinus wall. This happens by way of infectious, granulomatous or neoplastic disease, and by prothrombotic states. Often co-morbidities exist, with more than one factor predisposing to thrombus formation. Whether evaluating a neonate, infant, child or adolescent with CSVT, it is important to remember that upon clinical and laboratory investigation the majority will be found to have an underlying cause for thrombosis [1, 2, 4, 7] (Table 1).

The neonate is predisposed to CSVT by maternal factors (e.g., premature rupture of membranes, maternal infections and gestational diabetes), obstetrical trauma, hypoxic-ischemic encephalopathy, dehydration, infection and prothrombotic states. Calvaria molding from childbirth has been reported as a cause of superior sagittal sinus compression venous stasis and resultant thrombosis [8]. Calvaria fractures with resultant cortical vein or venous sinus

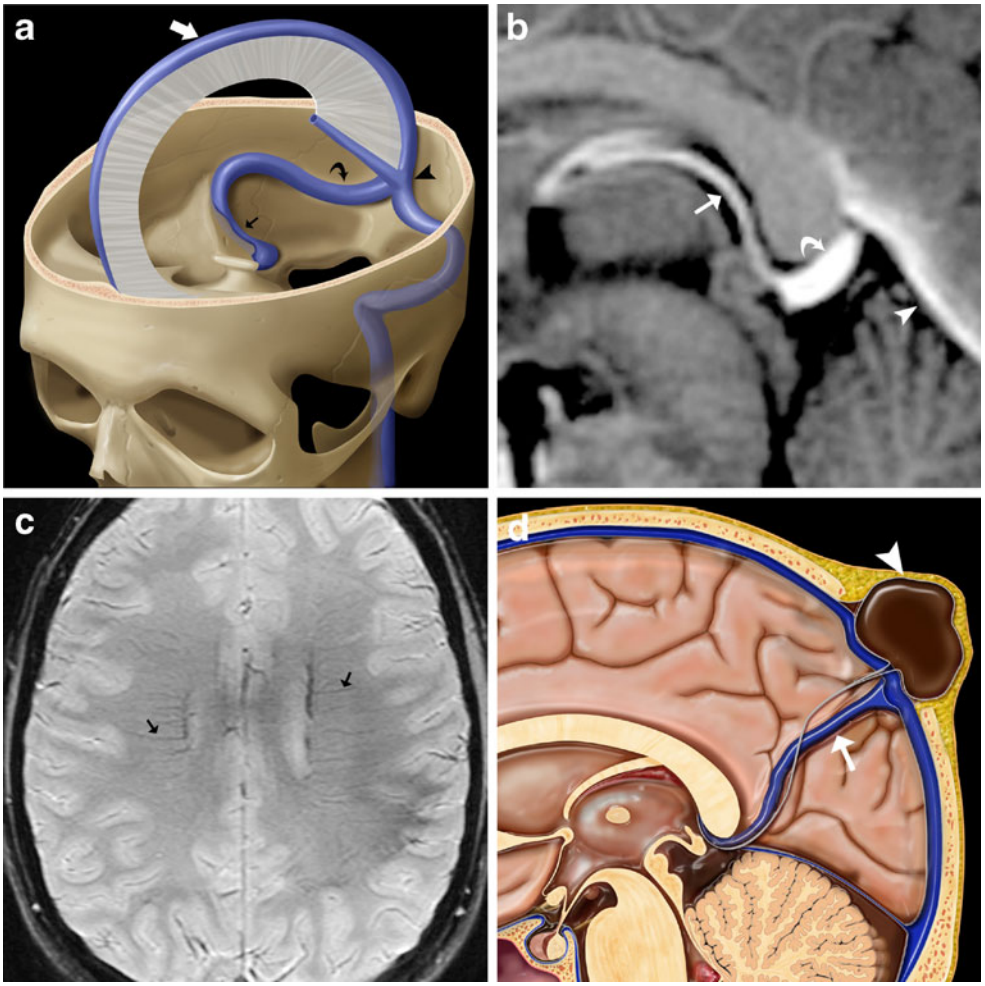

Fig. 1 Cerebral venous anatomy. **a** Color graphic of the normal cerebral dural venous sinuses. Superior sagittal sinus (*arrow*), right transverse sinus (*curved arrow*), torcular Herophili (*arrowhead*) and sigmoid venous sinus (*small arrow*). (Courtesy of Amirsys Publishing). **b** Normal enhanced 3-D spoiled gradient recalled (SPGR) MR venography (MRV). Sagittal image demonstrates homogeneous enhancement of the internal cerebral veins (*arrow*), Great cerebral vein or vein of Galen (*curved arrow*) and straight sinus (*arrowhead*). **c** Axial susceptibility-weighted MR image (SWI) demonstrates numerous normal medullary veins (*arrows*). **d** Persistent falcine venous sinus. Sagittal color graphic shows a vertically oriented falcine venous sinus (*arrow*). Note the associated vertex atretic parietal cephalocele (*arrowhead*). (Courtesy of Amirsys Publishing)

compression represent another mechanical cause of CSVT (Fig. 2). Asphyxia, dehydration, sepsis, bacterial meningitis, polycythemia and cardiac defects put the newborn and young infant at risk for CSVT. Prothrombotic factors encompass hematological and hypercoagulable states and have become increasingly recognized as important causes of CSVT. These include: factor V mutation, lupus anticoagulant and deficiencies of protein C, protein S, anti-thrombin-III and factor XII. Other disorders predisposing to CSVT include the prothrombin gene mutation, dysfibrinogenemia, sickle cell disease, disseminated intravascular coagulation and homocystinuria [3, 4, 7, 9].

In the older infant, child and adolescent, additional causal considerations include head and neck infections (e.g., otitis/mastoiditis/sinusitis) and cranial trauma (temporal-occipital fractures with sigmoid sinus occlusion) (Fig. 3). Less

Table 1 Causal factors in cerebral sinovenous thrombosis

Neonates	Infants and young children	Older children and adolescents
Dehydration	Dehydration	Dehydration
CNS infection	Infection	Infection
Gestational	• CNS	• CNS
• Maternal infection	• Head and neck	• Head and neck
• Gestational diabetes	Trauma	Trauma
• PROM	Iron deficiency anemia	Prothrombotic states
Obstetrical	Other prothrombotic states	Chronic systemic disease
• Trauma	Chronic systemic disease	Oral contraceptives
• Hypoxic ischemic injury	• Malignancy	
Prothrombotic states	• Chronic renal disease	
	• SLE	

PROM premature rupture of membranes, *CNS* central nervous system, *SLE* systemic lupus erythematosus

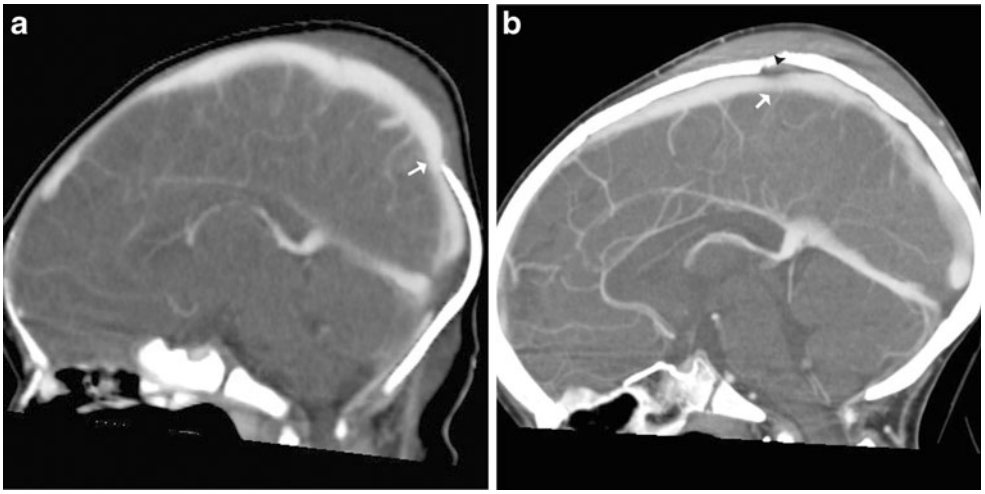

Fig. 2 Compression of the superior sagittal venous sinus. **a** Sagittal CT venography shows birth-related molding and compression of the superior sagittal venous sinus (*arrow*). **b** After closed head trauma, sagittal CT venography demonstrates compression of the superior sagittal venous sinus (*arrow*) resulting from depressed convexity skull fracture and associated epidural hematoma (*arrowhead*)

common causes of CSVT include chronic systemic disease (e.g., nephrotic syndrome, SLE, neoplasms), treatments for cancer (e.g., L-asparaginase) and oral contraceptives [2, 4, 10]. In my practice, I have found iron deficiency anemia to be an underappreciated cause of cerebral sinovenous thrombosis among infants and young children (Fig. 4) [14]. Taking all pediatric age groups into consideration at our children's medical center, trauma, dehydration, bacterial meningitis and iron deficiency anemia represent the most common causes of venous thrombosis.

In the setting of CSVT, brain parenchymal injury can result from venous backpressure leading to impaired parenchymal venous egress, with resultant venous hypertension, vasogenic and cytotoxic edema and possibly hemorrhagic

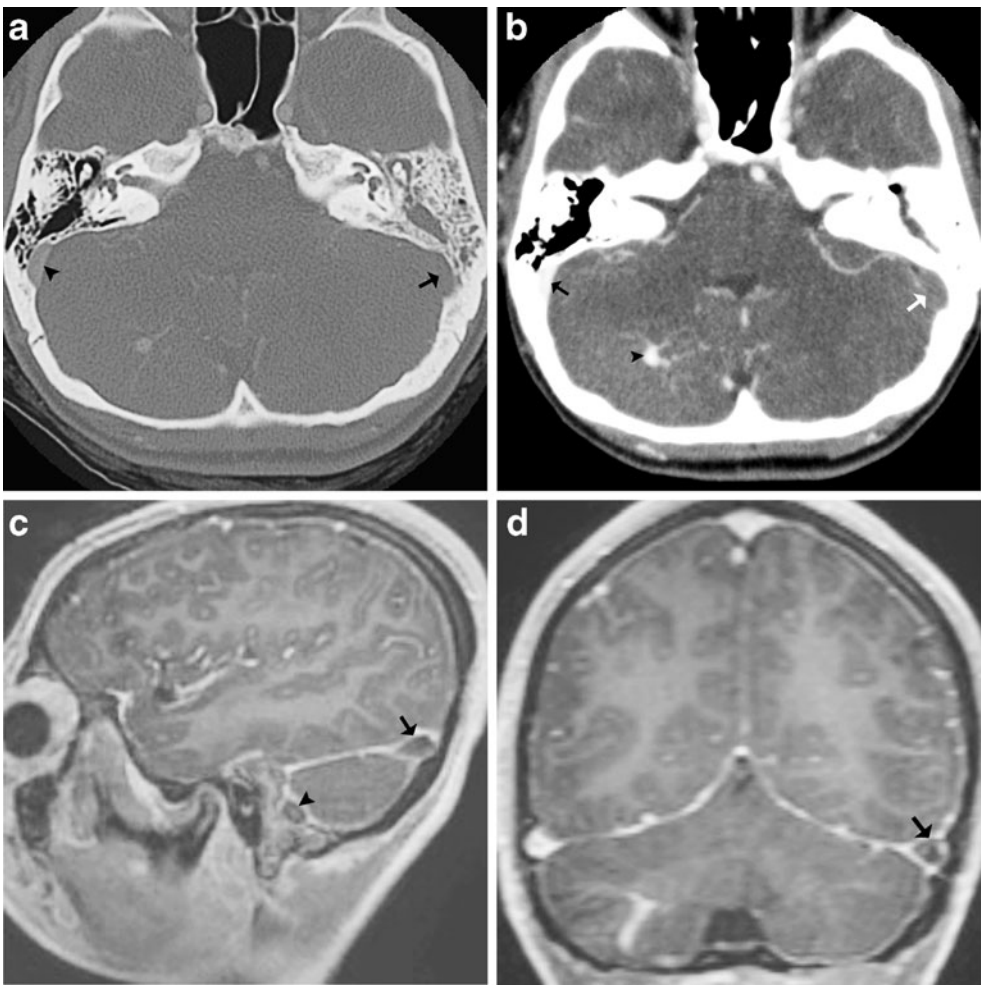

Fig. 3 Acute mastoiditis in a 14-year-old girl. **a** Axial contrast-enhanced temporal bone CT (bone detail) shows a lack of expected enhancement within the larger groove for the left sigmoid dural venous sinus (*arrow*). Note the normally enhancing smaller right sigmoid venous sinus (*arrowhead*). There is complete fluid opacification of the left middle ear and mastoid air cells. **b** Enhanced axial CT image with soft-tissue windowing confirms thrombus within the left sigmoid venous sinus (*white arrow*) and normal right sigmoid venous sinus (*black arrow*). Note the characteristic features of a developmental cerebellar venous anomaly (*arrowhead*). **c, d** Sagittal and coronal enhanced 3-D SPGR MRV images confirm thrombus at the junction between the lateral left transverse venous sinus and sigmoid sinus (*arrow*). The hypointense clot extends into the distal sigmoid venous sinus (*arrowhead*)

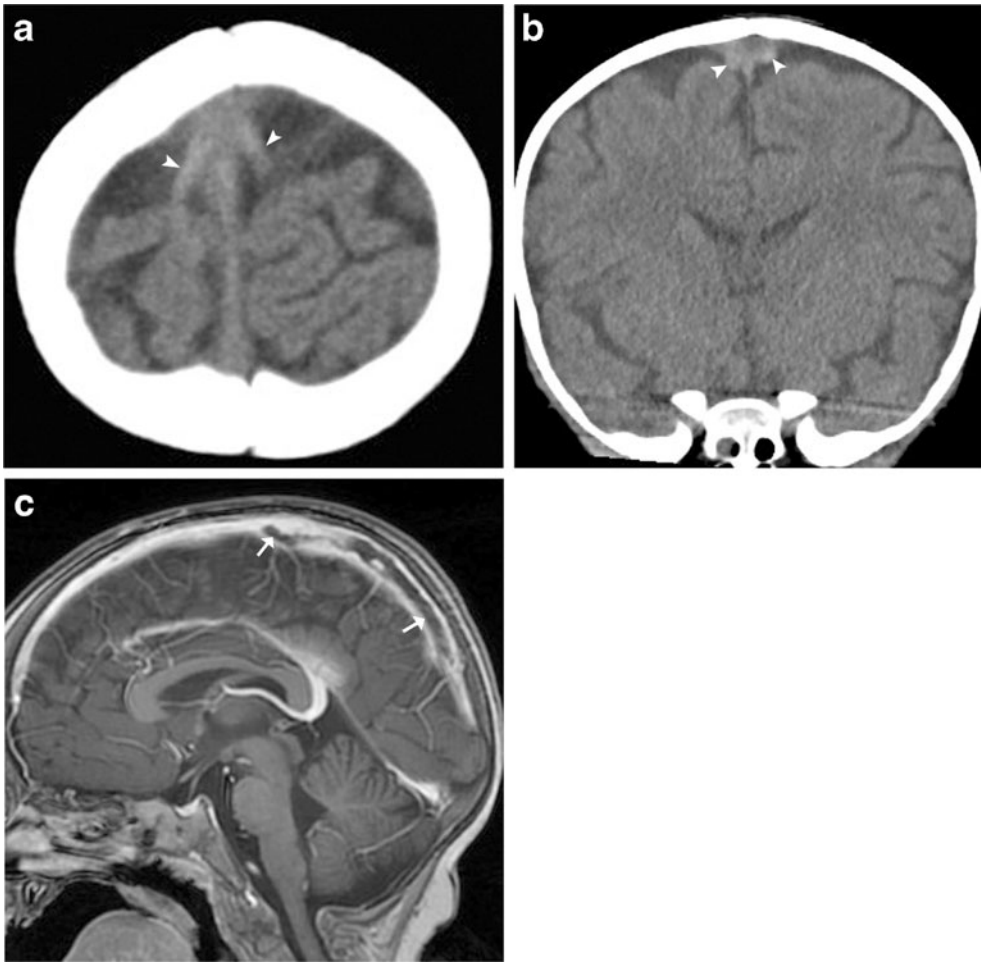

Fig. 4 Iron deficiency anemia and sinovenous thrombosis in a 7-month-old girl with seizures and vomiting. Axial unenhanced CT (**a**) and coronal CT reformation (**b**) show distention and increased attenuation of cortical veins (*arrowheads*). **c** Sagittal enhanced 3-D SPGR MRV confirms extensive hypointense thrombus within the superior sagittal venous sinus (*arrows*)

venous infarction (Fig. 5) [15]. The post-thrombotic complications of hydrocephalus and papilledema cause long-term morbidity [2, 4, 7, 9].

Some authors posit and testify to the fact that some infants and young children with CSVT have venous back pressure of such a magnitude to burst cortical dural veins, thus resulting in subdural hemorrhage (SDH) that mimics the SDHs found in abusive head trauma (AHT) [16, 17]. The quality of evidence to support this tenet is lacking [18–21]. Recently, McLean et al. [22] reported their observations of 36 patients ranging in age from birth to 19 years with proven CSVT. The authors reviewed cross-sectional brain imaging for the presence of SDH at the time of CSVT diagnosis. No SDH was detected among their CSVT cohort [22].

CT and CT venography

Radiologists enhance the imaging care of the child with intracranial venous thrombosis by recognizing predictive findings that lead to an accurate and timely diagnosis. Often the clinical history is vague or lacking altogether or perhaps pointing the clinician and imaging physician toward another diagnosis [7].

Tang et al. [23] reported that in patients ultimately proved to have CSVT, the clinical history as stated on the imaging study order raised concern of thrombosis in only 5% of CTs and 33% of MRI examinations. They also showed that when the clinical indication for the cranial CT study reflected no suspicion for CSVT, the false-negative rate for detecting thrombosis on the unenhanced brain CT was 53% [23].

The unenhanced CT of the normal newborn and young infant brain shows the attenuation of the superior sagittal venous sinus to be subtly greater than that of adjacent cerebral gray matter (Fig. 6). Additionally, in these young patients, the cortical dural veins and deep venous structures should be iso-attenuating to slightly hyper-attenuating to the unenhanced cortex. In the older infant, child and adolescent the dural venous sinuses and deep midline venous structures are normally hypo- or iso-attenuating to gray matter. Generally speaking, beyond the neonatal period and first few months of infancy, the dural venous sinuses, cortical dural veins and deep venous system are normally relatively inconspicuous [1, 2, 24, 25].

The characteristic unenhanced CT appearance of cerebral sinovenous thrombosis is the presence of hyper-attenuating thrombus within the superficial, deep or dural venous sinuses. When the radiologist observes increased attenuation within

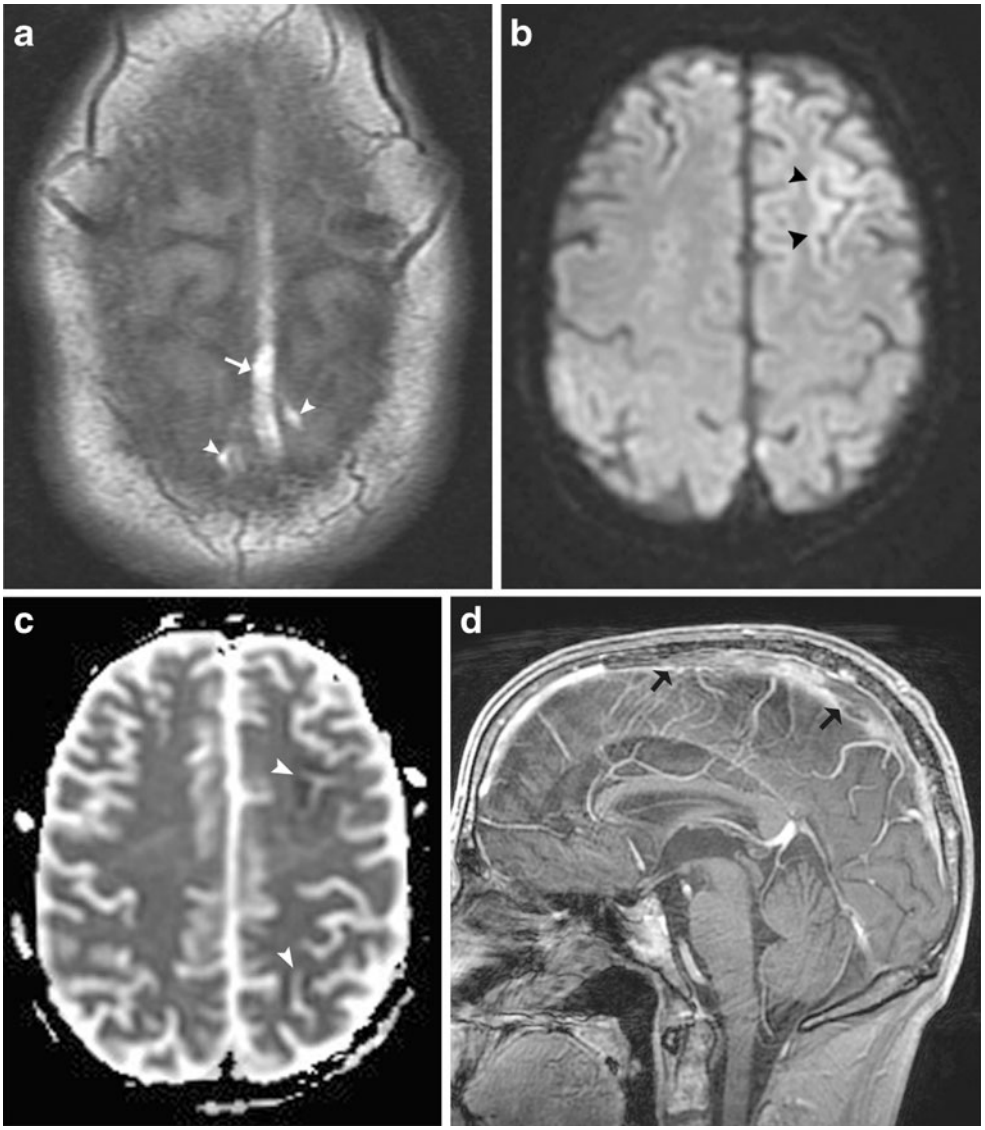

Fig. 5 Sinovenous thrombosis and cerebral edema in a 15-year-old boy with leukemia being treated with L-asparaginase; he had new-onset seizures. **a** Axial T1-weighted image shows hyperintense thrombus within the superior sagittal venous sinus (*arrow*) and adjacent cortical veins (*arrowheads*). **b** Axial diffusion-weighted image shows left frontal lobe cortical and subcortical hyperintensity (*arrowheads*). **c** ADC image confirms left frontal and parietal regions of reduced cortical diffusivity (cytotoxic edema) (*arrowheads*). **d** Sagittal enhanced 3-D SPGR MRV confirms thrombus within the superior sagittal venous sinus (*arrows*)

cortical veins, superior and inferior sagittal sinuses or the deep midline venous structures (internal cerebral veins, vein of Galen, and straight sinus) then CSVT should be considered. Segmental regions of increased attenuation within the dural venous sinuses are also a hint to the presence of CSVT. Distention of a dural venous compartment irrespective of the

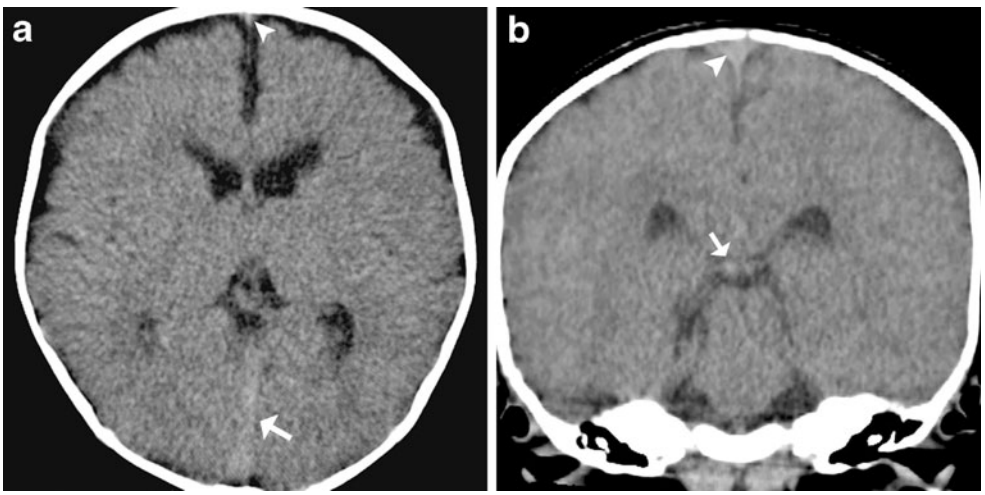

Fig. 6 Normal neonatal unenhanced venous anatomy. **a** Axial unenhanced CT image shows normal subtle increase in straight sinus attenuation (*arrow*). Also note the normal increased attenuation of the anterior inferior aspect of the superior sagittal venous sinus (*arrowhead*). **b** Coronal unenhanced CT reformation in the same patient shows normal, slightly hyper-attenuating internal cerebral veins (*arrow*) and superior sagittal venous sinus (*arrowhead*)

intrinsic attenuation or signal intensity is a clue to the diagnosis of venous sinus thrombosis (Fig. 7) [23–28]. Radiodense dural venous sinuses might reflect elevated hematocrit and mimic thrombosis [29]. If the intracranial venous and arterial structures appear similarly high in attenuation, then suspect primary or secondary polycythemia as the cause. This appearance of dense venous and arterial structures is an ominous sign (hyperviscosity) and warrants immediate clinical attention [29].

Historically, many imaging observations associated with CSVT have been well described on unenhanced and enhanced CT and are embraced by radiologists as being critical to a strongly suspected diagnosis of thrombosis. On unenhanced CT imaging, the cord sign (high attenuation of the cortical vein) and the hyperdense dural sinus sign, or dense dural sinus sign, are findings supporting the diagnosis of SVT [1, 2, 25, 27, 28]. Contrast-enhanced CT and CT venography show the empty delta sign in the setting of superior sagittal sinus thrombosis (Fig. 8). Although dogma continues to prevail upholding these CT signs as being key to making a timely and accurate diagnosis of thrombosis, the truth is that the sensitivity of these CT signs is variable, ranging from 5% for the cord sign to 20% for the dense dural sinus sign to 70% for the empty delta sign [25, 30, 31]. Thus, a normal-appearing unenhanced CT should not dissuade the radiologist from proceeding to either CT venography or MRI and MR venography (MRV) if clinically warranted.

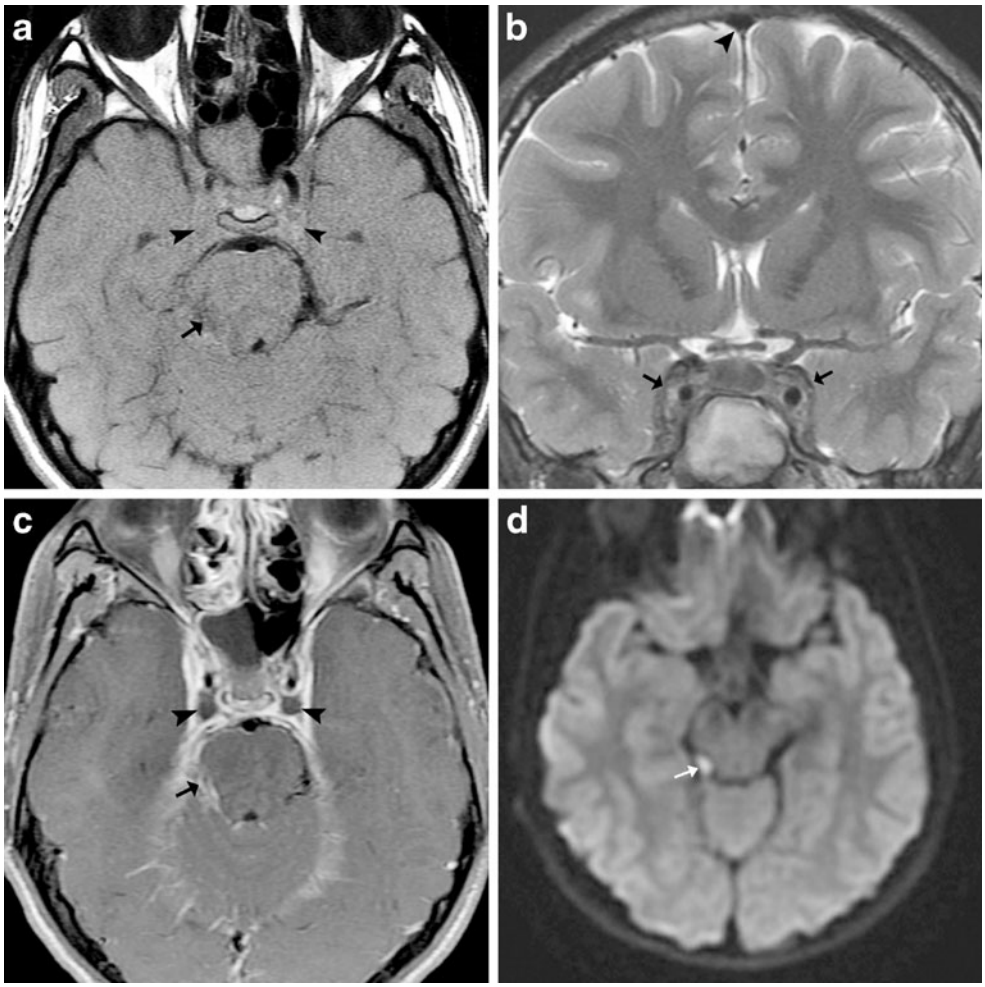

Fig. 7 Bilateral cavernous sinus thrombosis secondary to sphenoid sinusitis. **a** Axial T1-weighted MR image shows distention of the cavernous sinuses (*arrowheads*). The signal intensity of the cavernous sinus is nearly isointense to gray matter. Normally the cavernous sinus is predominantly hypointense on T1-weighted imaging prior to intravenous contrast administration. Note the obliteration of the right perimesencephalic cistern and hypointensity in the mesencephalon secondary to associated meningitis and edema (*arrow*). **b** Coronal T2-weighted image demonstrates distention of the cavernous sinuses and heterogeneity of signal secondary to thrombus (*arrows*). There is normal hypointensity of blood within the superior sagittal venous sinus (*arrowhead*). **c** Axial T1-weighted IV contrast-enhanced MR image with fat saturation demonstrates hypointense thrombus within the cavernous sinuses (*arrowheads*). There is thickening and strong enhancement of the lateral cavernous sinus dura. Also, note the focal enhancement of the right perimesencephalic cistern, a result of associated meningitis (*arrow*). **d** Axial trace diffusion-weighted image shows a linear focus of diffusion hyperintensity within the right perimesencephalic cistern, presumed to represent thrombus within the right basal vein of Rosenthal (*arrow*)

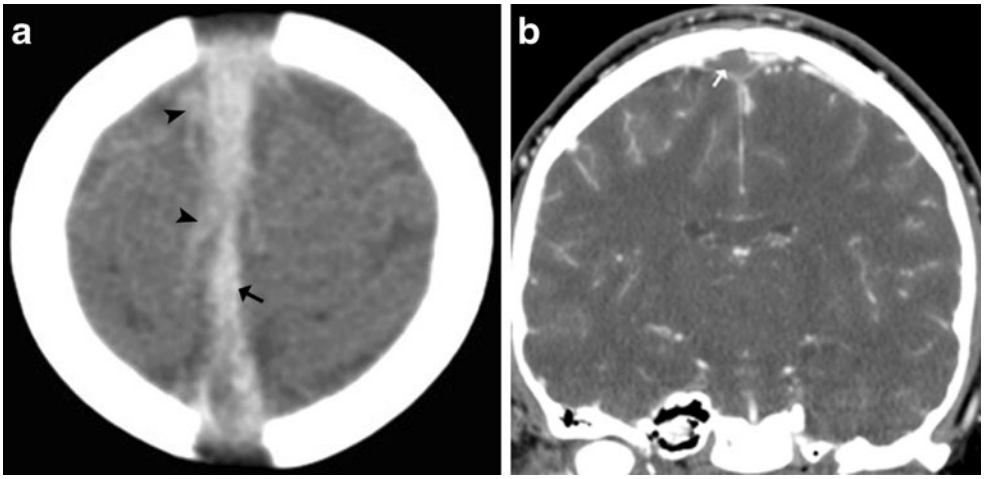

Fig. 8 CT signs of sinovenous thrombosis. **a** Axial unenhanced CT image through the cerebral convexity shows hyper-attenuating cortical dural veins (cord sign) (*arrowheads*) and the dense dural venous sinus sign (*arrow*). **b** Coronal enhanced CT image shows hypo-attenuating thrombus (*arrow*) filling the superior sagittal venous sinus (empty delta sign)

The normal lower brain attenuation of the newborn and young infant, the relatively higher normal hematocrit, and the less deformable red blood cells (RBCs) of these patients compared with the adult might lead the radiologist to consider the differential diagnosis of hemoconcentration versus sinovenous thrombosis when reviewing unenhanced brain CT studies. In large part, it is our gestalt of the imaging findings based upon our experience in neuroimaging that either comforts us to render a normal impression or raises suspicion, thus leading to a contrast-enhanced study. An accurate clinical history will heighten our concern. Does the patient have a clinical risk for cerebral venous thrombosis (known malignancy or a history of previous thrombotic events such as pulmonary thromboembolism)? As a pediatric radiologist, I entertain the possibility of sinovenous thrombosis if the clinical history is suggestive of the diagnosis or if the unenhanced CT demonstrates age-inappropriate attenuation of the intracranial venous system, including signs of increased attenuation of convexity cortical veins, hyper-attenuation of the internal cerebral veins and other midline venous structures, and an appearance of greater than expected attenuation among segments of the dural venous sinuses. Additionally, unexplained parenchymal edema or subcortical hemorrhage should also lead the radiologist to consider cerebral venous thrombosis in the differential diagnosis. These observations should prompt the referring physician to proceed with CT venography or MRI and MRV immediately [1, 2, 31].

Black et al. [32] reaffirm the importance of differentiating hematocrit (hemoconcentration) effect from sinovenous thrombosis. In their study of pediatric and adult patients proved not to have sinovenous thrombosis, all had dural venous sinus Hounsfield unit valves (HU) of 70 or less (measured at the torcular Herophili). The authors warn that aging, recanalizing clot could yield an HU value less than 70 and thus lead to a false-negative interpretation on unenhanced CT [32]. To address this false-negative risk, the authors observed that when clot is iso- or hypo-attenuating to normal brain (anemia and aging clot), the ratio of hematocrit-to-dural venous sinus HUs (H:H) might be helpful in diagnosing CSVT [32] (Fig. 9). The mean H:H

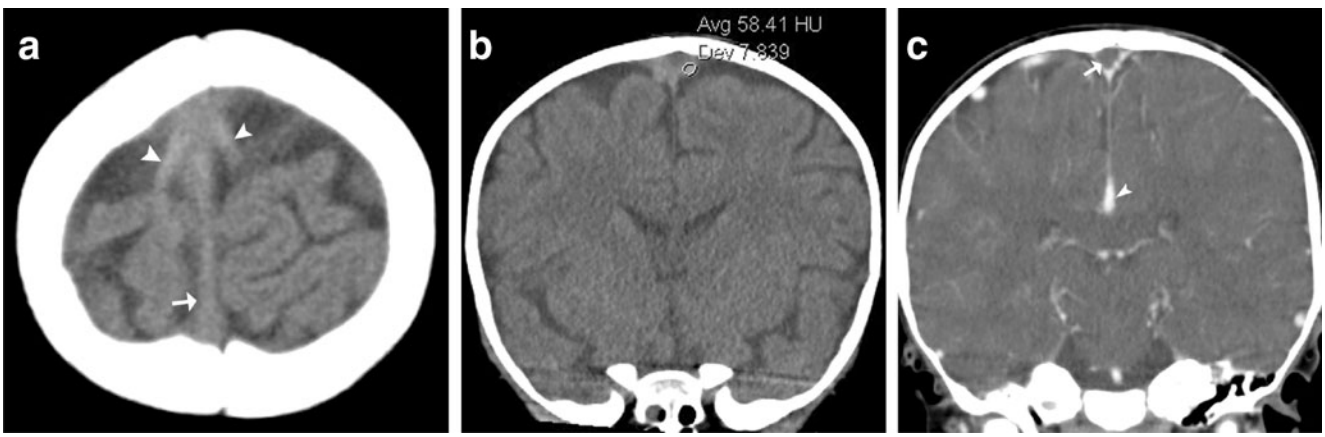

Fig. 9 Iron deficiency anemia and sinovenous thrombosis in a 10-month-old girl with lethargy and new onset of generalized seizures. **a** Axial unenhanced CT image shows distention and increased attenuation of cortical dural veins (*arrowheads*). The superior sagittal sinus appears normal (*arrow*). **b** Coronal CT reformation shows a CT HU measurement within the superior sagittal sinus of 58. The calculated H:H is 2.0. This is highly suspicious for thrombus within the superior sagittal venous sinus. **c** Coronal contrast-enhanced CT shows the empty delta sign (*arrow*). Note the normal enhancing inferior sagittal venous sinus (*arrowhead*)

Table 2 Parameters for helical multidetector CT venography

Contrast type: iopamidol 370
(Isovue 370, Bracco Diagnostics, Princeton, NJ)
Dosage: 2 ml/kg
Injection rate: 2 ml/s
Scan delay: 2 min
mA/kVp
• 0-5 years 100 kV, mA by automatic tube current modulation
(min. mA 80, max. mA 140)
• >5 years 120 kV, mA by automatic tube current modulation
(min. mA 80, max. mA 160)
Axial helical acquisition
Coronal and sagittal reformatted MIP images

A Toshiba Aquilion 64 (Toshiba Medical Systems, Irvine, CA) multidetector CT system was used

MIP maximum intensity projection

among Black et al.'s [32] normal subjects was ≤1.4. Among patients proved to have CSVT it was 2.2 or greater. H:H from the dural venous sinus equaling 1.4–2.2 should be viewed with concern and strong consideration given to further imaging (CT venography or MRV) [32, 33]. A recent clinical and imaging investigation at the University of Utah of adult patients with proven CSVT showed dural venous sinus HU measurements greater than 70 or H:H ratios of 1.9 or greater. In patients with HUs <52 or H:H <1.4 no thromboses were found. One-third of patients proved to have CSVT had H:H between 1.4 and 1.9 (personal communication by David Besachio, DO, presented at the American Society of Neuroradiology, 50th annual meeting, New York, April 24, 2012). To date, these HU thresholds and H:H ratios have not been validated in a pediatric population with CSVT.

In many centers, CT venography is the most commonly used test when patient risk factors, clinical symptoms, or the unenhanced CT suggests CSVT (Table 2). I rely on CT venography to follow unenhanced CT in the initial evaluation of suspected CSVT (Fig. 10). False-positive CT venography examinations can lead to inappropriate therapy. The combination of the strongly enhancing normal vascularized inner dural border zone of the dural venous sinus in the neonate and young infant and relatively less attenuating (compared with the enhancing dura) contrast-containing blood within the dural venous sinus can mimic sinovenous thrombosis [34]. In cases such as this, supplemental cranial sonography with color and pulsed Doppler have improved my diagnostic accuracy and avoided inappropriate therapy (Fig. 11) [35]. Supplemental cranial sonography is most applicable in the neonate and young infant for the investigation of midline venous structures including the superior and inferior sagittal venous sinuses, internal cerebral veins, vein of Galen and straight sinus. If the neonate or young infant's CT venography is strongly suggestive of CSVT and US is also abnormal, then treatment for CSVT should begin immediately. In these patients, I also make every effort to perform brain MRI and IV-enhanced MRV within 24 h to assess for brain parenchymal abnormalities (edema, ischemia and hemorrhagic infarction) and to map the extent of thrombus [1, 2, 6]. Alternatively, if the clinical symptoms, signs and complementary US with color and pulsed Doppler are discordant with the CT venography results, I move immediately to MRI and enhanced MRV as the gold standard for CSVT detection. In older children and adolescents, CT venography is very satisfactory in quickly confirming the

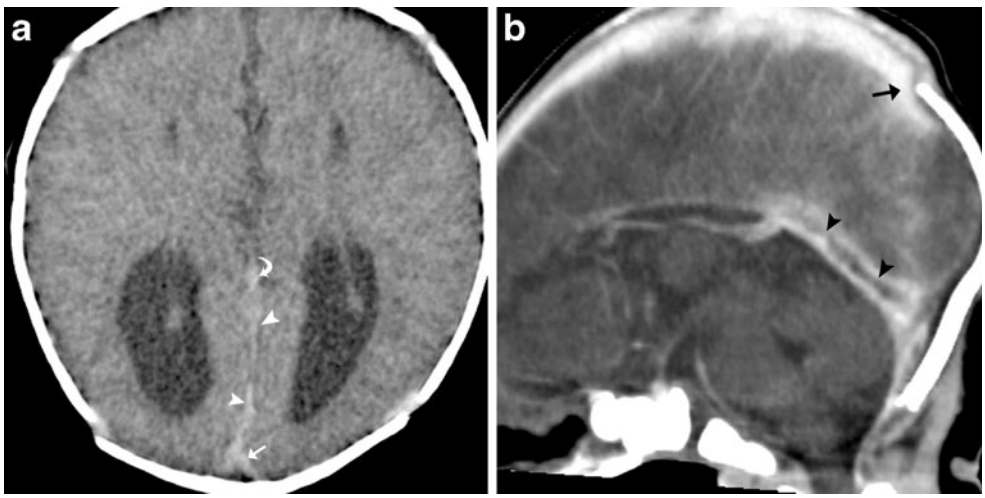

Fig. 10 Sinovenous thrombosis: value of CT venography. Images in a newborn known to have agenesis of the corpus callosum who presented with seizures. **a** Axial unenhanced CT shows increased attenuation within the great cerebral vein or vein of Galen (*curved arrow*), straight sinus (*arrowheads*) and torcular Herophili (*arrow*). **b** Sagittal reformation from CT venography shows linear hypo-attenuating thrombus (*arrowheads*) within the straight sinus. Note the compression of the superior sagittal venous sinus caused by calvaria molding (*arrow*)

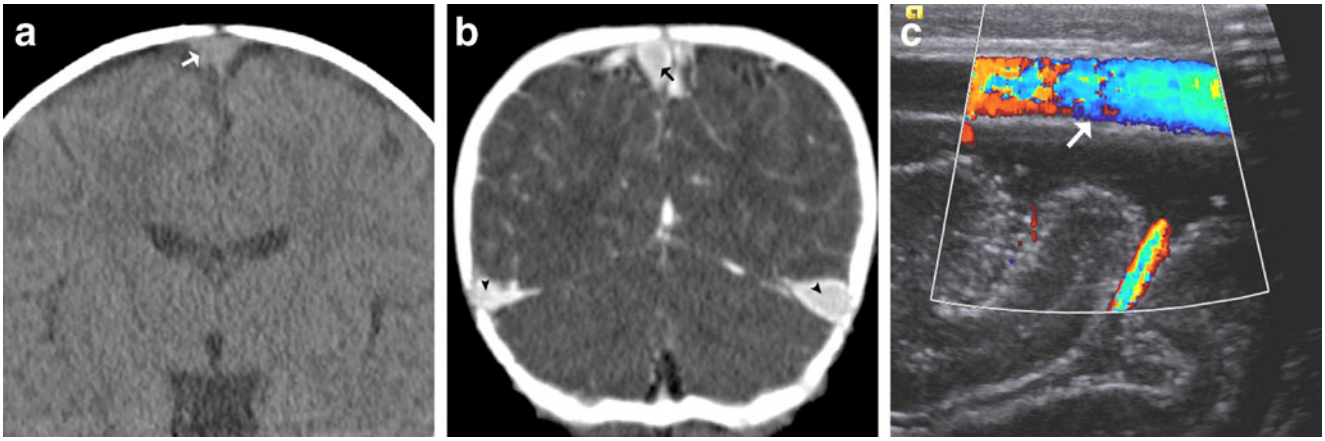

Fig. 11 Pseudosinovenous thrombosis in a 12-month-old girl with macrocephaly. **a** Coronal reformation from unenhanced CT shows homogeneous slightly hyper-attenuating superior sagittal sinus (*arrow*). **b** Coronal reformation from CT venography demonstrates low-attenuation regions within the central superior sagittal venous sinus (*arrow*) and lateral transverse venous sinuses (*arrowheads*). The presence of a cardiac pacemaker precluded MRI and MRV. **c** Sagittal cranial color Doppler imaging immediately following the CT venography confirms normal venous flow throughout the superior sagittal venous sinus (*arrow*)

diagnosis of CSVT. The presence of associated seizures, encephalopathy, hydrocephalus and parenchymal hemorrhage in the setting of CSVT calls for expeditious MRI and enhanced MRV. Another false-positive CT pitfall is seen in the setting of temporal or occipital bone fractures associated with acute extradural hemorrhage lateral to the sigmoid venous sinus. This extradural hemorrhage can compress the venous sinus and mimic SVT. CT venography including coronal reformations distinguishes a compressed from a thrombosed dural venous sinus (Fig. 12). Parafalcine and paratentorial subdural hemorrhage might be misinterpreted as SVT. The routine use of axial helical CT followed by coronal and sagittal CT reformations helps in making the distinction. Occasionally, thrombus within the inferior sagittal venous sinus is misinterpreted as an acute intradural hemorrhage (Fig. 13). Dural venous sinus fenestrations and arachnoid granulations represent other potential causes of false-positive enhanced CT examinations and are discussed further under the topic of MRI/MRV false-positive pitfalls [25, 26].

MRI and MRV

The appearance of CSVT on unenhanced MRI studies is often complex, being influenced by clot age, location and extent of thrombus, whether the clot is partly or completely

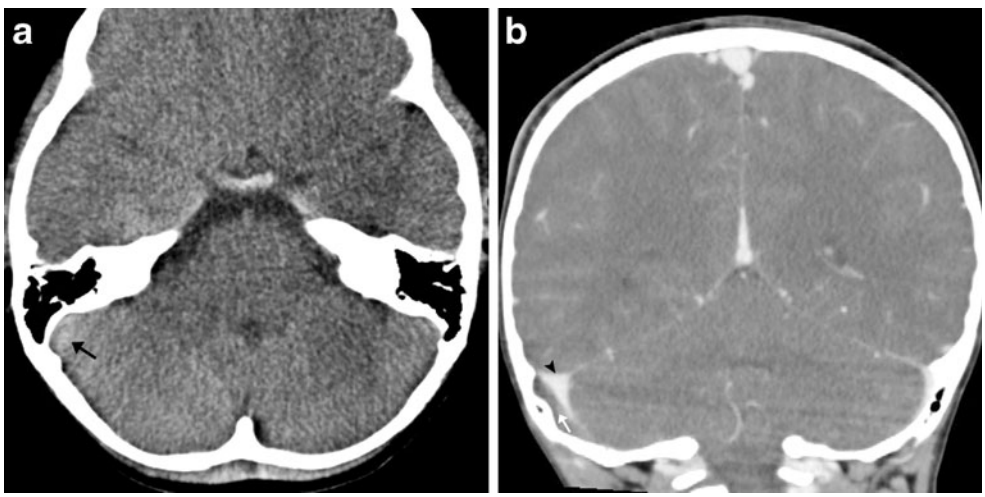

Fig. 12 Extradural hemorrhage mimics venous thrombosis in a 15-year-old boy with blunt trauma to the right temporal occipital region. **a** Axial unenhanced CT shows increased attenuation within the right sigmoid vascular groove (*arrow*). This was interpreted as being suggestive of thrombus within the right sigmoid venous sinus. **b** Coronal reformation following CT venography demonstrates medial displacement of the proximal right sigmoid sinus by extradural hemorrhage (*white arrow*). Note the normal enhancing displaced sigmoid dural venous sinus (*black arrowhead*)

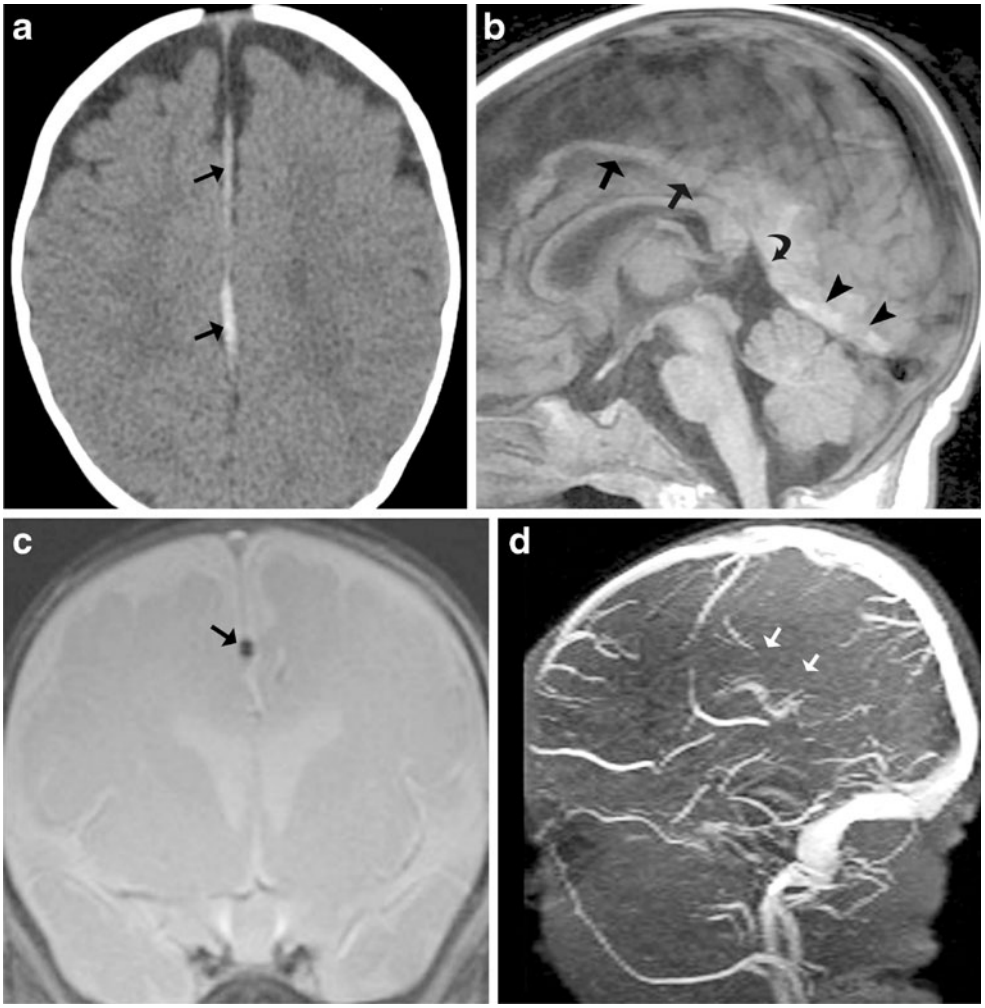

Fig. 13 Thrombosis of the inferior sagittal sinus mimics intradural falcine (subdural) hemorrhage. **a** Axial unenhanced CT image shows high-attenuation thrombus in the anatomical position of the inferior sagittal venous sinus (*arrows*). This had been interpreted as subdural hemorrhage as might be seen in abusive head trauma. **b** Sagittal T1-weighted MR image shows hyperintense thrombus within the inferior sagittal sinus (*arrows*), the great cerebral vein or vein of Galen (*curved arrow*) and straight sinus (*arrowheads*). **c** Coronal GRE demonstrates hypointense thrombus throughout the inferior sagittal venous sinus (*arrow*). **d** Two-dimensional TOF unenhanced MRV shows a lack of flow signal in the expected position of the inferior sagittal venous sinus (*arrows*)

occlusive, clot hydration, clot serum separation, MR sequences employed, and magnetic field strength [36–38]. Intraluminal clot evolves in stages that parallel extravascular clot.

The normal unenhanced intracranial dural venous sinuses on spin-magnitude MRI show hypointensity within the sinuses on T1-weighted sequences, hypointensity on T2-weighted sequences, hyperintensity on normal gradient recall imaging (GRE) and hypointensity on fluid inversion recovery sequences (FLAIR). On normal unenhanced MRI sequences, slow venous flow, in-plane venous flow, and entry-slice phenomena can mimic the presence of venous clot [1, 25, 26]. This is particularly common in neonates and children younger than 2 years [1, 2, 25, 26, 29]. The addition of a coronal GRE sequence is often critical in detecting the paramagnetic susceptibility effects of hemoglobin breakdown products. The GRE sequence remains particularly helpful in the detection of thrombus when clot is isointense on T1-weighted imaging or hypointense on T2-weighted sequences [38, 39]. Another important sequence modification to consider in the routine MR brain examination is the extension of unenhanced sagittal T1-weighted imaging to the lateral-most margins of the brain; this often aids in the detection of hyperintense subacute thrombus within the transverse and sigmoid venous sinuses. T1-weighted imaging in the early and late subacute stages of dural venous thrombosis shows T1 hyperintensity as a result of extracellular methemoglobin. A subtle sign of CSVT might be cortical and deep intracranial veins appearing hyperintense on T1-weighted sequences [26, 40, 41]. As with intravenous-enhanced CT, detecting a dural venous sinus filling defect with enhanced MRI and/or MRV confirms the diagnosis of CSVT (Fig. 14) [1, 2, 6, 36–39].

The presence of partial or chronic thrombus (>15 days of age) represents a potential cause of false-negative CT and MR interpretations. On the unenhanced MRI the heterogeneity of MR signal from chronic recanalizing clot can mimic normal slow-moving venous blood [42]. The utilization of GRE imaging, SWI, and 3-D enhanced MRV improves diagnostic accuracy in such cases (Fig. 15) [25, 26]. Susceptibility-weighted imaging (SWI) is sensitive to minute amounts of hemosiderin and ferritin. SWI is more sensitive than GRE to detect microbleeds. However, SWI displays normal and clot-containing veins and dural venous

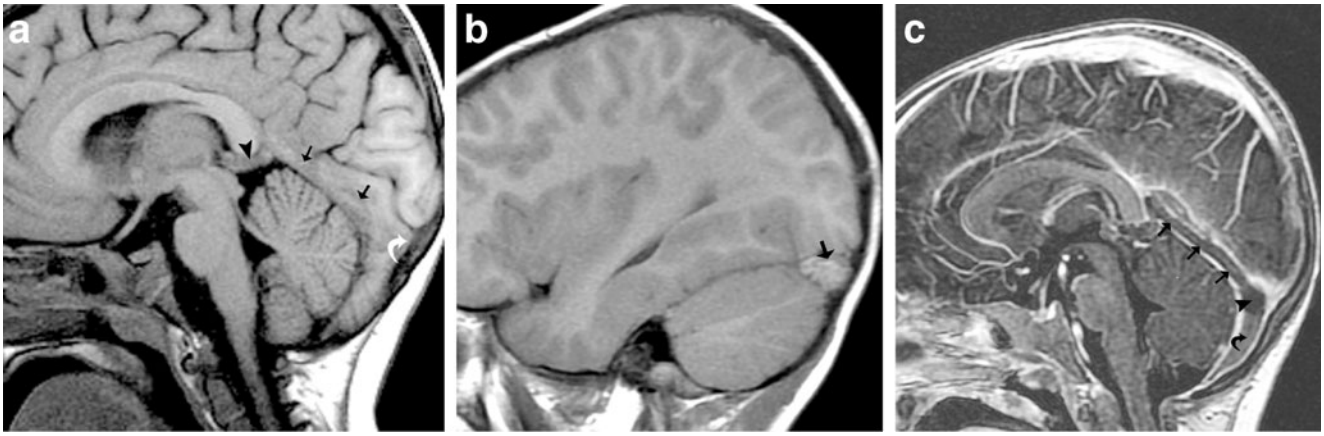

Fig. 14 MRI and MRV of cerebral sinovenous thrombosis in an 8-year-old girl with encephalopathy. **a** Sagittal T1-weighted MR image shows thrombus isointense to brain parenchyma within the great cerebral vein or vein of Galen (*arrowhead*), straight sinus (*arrows*), and torcular Herophili (*curved arrow*). Note the increased T1 signal inferior to the torcular Herophili clot, which represents thrombus within a persistent occipital dural venous sinus. **b** Sagittal T1-weighted image through the dominant right transverse venous sinus shows lateral transverse venous sinus extension of hyperintense thrombus (*arrow*). **c** Sagittal enhanced 3-D SPGR MRV image shows hypointense thrombus throughout the straight sinus (*arrows*), torcular Herophili (*arrowhead*), and persistent midline occipital dural venous sinus (*curved arrow*)

sinuses as hypointense structures, thus potentially leading to a false-negative interpretation of the MRI study when clot is present within the venous structures [43]. Therefore, GRE in my practice has not been supplanted by SWI. Additionally, I have found it helpful when initiating my routine MRI search pattern to spend a few moments reviewing the 2-D GRE MR

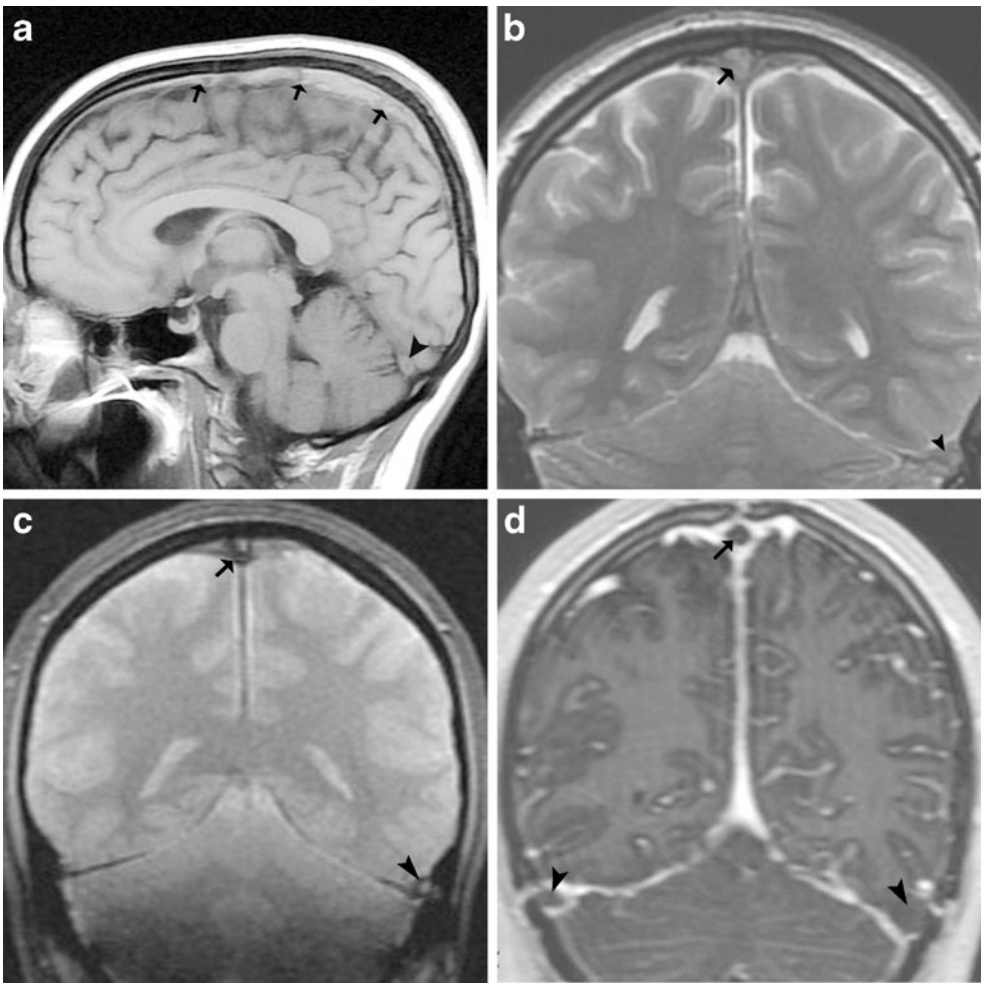

Fig. 15 Chronic sinovenous thrombosis in a 16-year-old girl taking oral contraceptives and suffering from worsening headaches who presented with focal seizure. **a** Sagittal T1-weighted MR image shows hyperintense thrombus throughout the superior sagittal sinus (*arrows*). Note the hyperintensity within the torcular Herophili (*arrowhead*). **b** Coronal T2-weighted MR image demonstrates hyperintense clot within the superior sagittal venous sinus (*arrow*) and left lateral transverse venous sinus (*arrowhead*). **c** Coronal GRE image demonstrates the paramagnetic effect of thrombus within the superior sagittal venous sinus (*arrow*) and the left lateral transverse venous sinus (*arrowhead*). The right transverse venous sinus was interpreted as being hypoplastic. **d** Coronal reformation from 3-D SPGR enhanced MRV shows hypointense thrombus within the superior sagittal sinus (*arrow*) and bilateral transverse venous sinuses (*arrowheads*)

scout localizers, evaluating for normal venous sinus flow, which appears as hyperintense signal [21, 22]. These scout data are under-utilized by radiologists and trainees alike.

Brain parenchymal changes in the setting of CSVT are common and much better appreciated with MR than CT. The spectrum of parenchymal findings includes reversible vasogenic edema (increased ADC values), cytotoxic edema (decreased ADC values) and subcortical hemorrhagic infarction (Figs. 5, 7 and 16) [44–46]. Fortunately, unlike pediatric arterial strokes, the edematous parenchymal abnormalities of SVT are often reversible [45, 46]. Unexplained focal cerebral edema and subcortical parenchymal hemorrhage should prompt the consideration of CSVT [1, 2, 6, 15]. This is particularly true for deep thalamic edema that can arise from internal cerebral vein thrombosis (Fig. 16).

Venous flow is a common source of false-positive TOF MRV studies, specifically the saturation effect from in-plane slow venous flow that comes about when venous flow is parallel to the imaging acquisition. The resultant flow gap can simulate venous sinus atresia, hypoplasia or thrombosis. Blood signal intensity on TOF venography is greatest when the imaging acquisition plane is perpendicular to venous flow. Additionally, the use of an inferior saturation band (to saturate arterial inflow) often leads to signal loss within the anterior aspect of the superior sagittal venous sinus (because of the cephalad direction of flow). Venous sinus hypoplasia (seen in approximately 30% of normal patients), venous sinus septations and arachnoid granulations can represent sources of false-positive TOF MRV studies [25, 26, 47–50].

Arachnoid granulations and venous sinus septations can mimic the appearance of sinovenous thrombosis. Arachnoid granulations are normal anatomical structures that play an important role in CSF resorption (particularly in the first 2 years of life) and are particularly common in the superior sagittal sinus, torcular Herophili and transverse dural venous sinuses. Their normal protrusion into the venous sinus can mimic thrombus. This is particularly true of imaging in the short axis of the dural venous sinus. When imaged in the long axis, arachnoid granulations have a round morphology

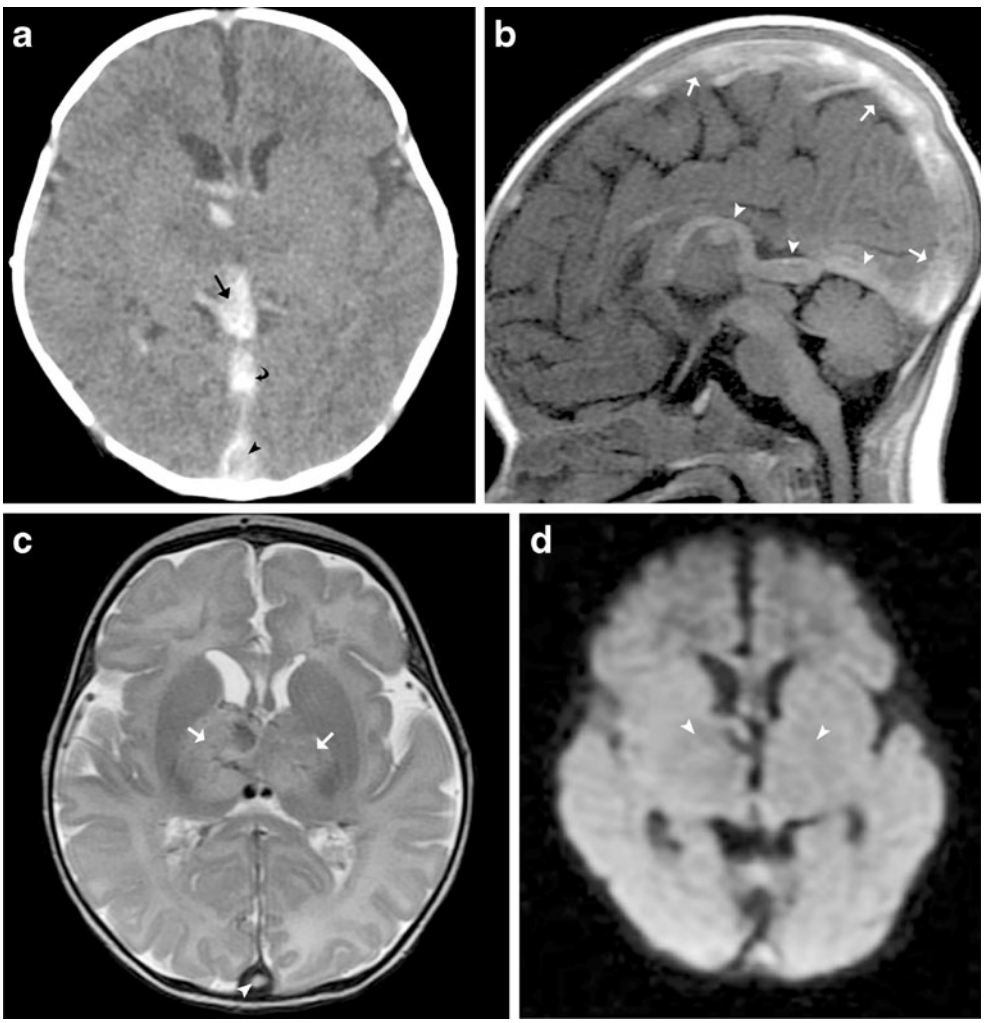

Fig. 16 Basal ganglia edema and hemorrhage secondary to cerebral sinovenous thrombosis in a 6-month-old girl with profound iron deficiency anemia, lethargy and seizures. **a** Axial unenhanced CT shows hyperattenuating midline venous thrombus involving the great cerebral vein or vein of Galen (*arrow*), straight sinus (*curved arrow*) and torcular Herophili (*arrowhead*). Also note the low-attenuation basal ganglia edema and focal right basal ganglia hemorrhage. **b** Sagittal T1-weighted MR image shows hyperintense thrombus within the superior sagittal sinus (*arrows*), the internal cerebral veins, vein of Galen and straight sinus (*arrowheads*). **c** Axial T2-weighted MR image demonstrates hyperintense basal ganglia signal representing edema (*arrows*). Note the hyperintense clot within the posterior aspect of the superior sagittal venous sinus (*arrowhead*). **d** Axial diffusion-weighted image shows increased diffusivity consistent with vasogenic edema within the basal ganglia (*arrowheads*). Vasogenic edema is common in the setting of cerebral sinovenous thrombosis

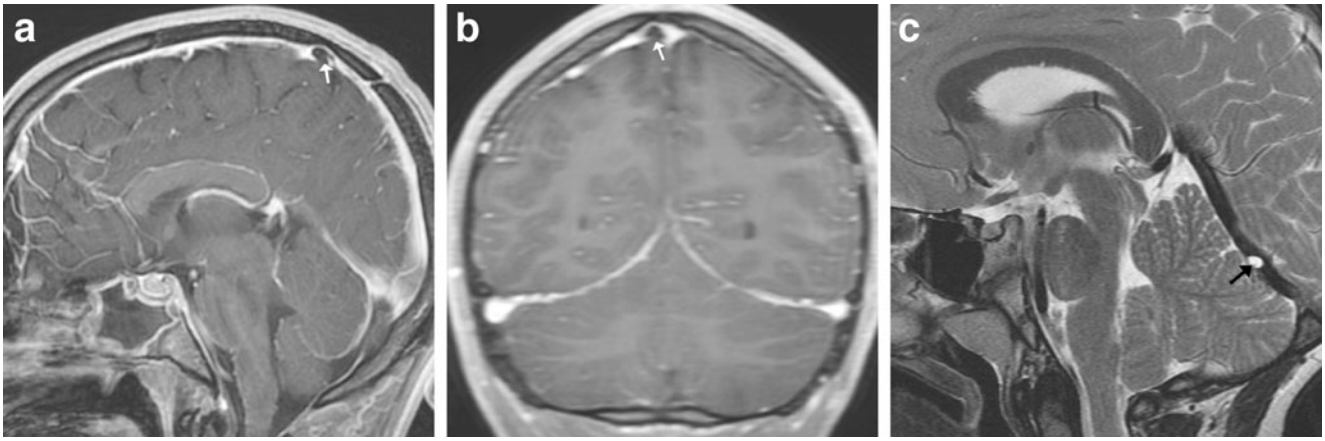

Fig. 17 Normal arachnoid granulations. **a** Sagittal and (**b**) coronal enhanced T1-weighted MR images demonstrate a round filling defect within the superior sagittal venous sinus characteristic of a normal arachnoid granulation (*arrows*). Note the opacified sphenoid sinus with intense mucosal enhancement (sinusitis). **c** Sagittal T2-weighted MR image from another patient shows a characteristic round hyperintense arachnoid granulation protruding into the straight sinus (*arrow*). Arachnoid granulations should follow CSF signal intensity

and have attenuation and signal intensity that mirrors CSF (Fig. 17) [50].

A source of false-negative TOF MRV is the presence of clot within the dural venous sinus that exhibits T1 shortening or hyperintensity, thus mimicking the presence of venous sinus flow or T1 shine-through [25, 26]. Recognizing that some children will be non-sedate, or orally sedated and have no IV access, the pitfalls of TOF MRV can be mitigated by avoiding the axial plane of image acquisition, avoiding the use of an inferior saturation pulse, and in suspect regions applying the phase-contrast venography technique [25, 26, 47–50].

Intravenous contrast-enhanced 3-D MRV (because of the reduced spin saturation effects of the gadolinium chelate) has become the MRV standard for the detection and characterization of CSVT. At my institution, we use an intravenous contrast-enhanced sagittal 3-D SPGR technique with isotopic coronal and axial reformations (Table 3). It circumvents the flow-related artefacts and T1 shine-through pitfalls inherent with 2-D unenhanced TOF MRV. This enhanced technique better differentiates between atretic and hypoplastic sinuses and is more sensitive to detecting non-occlusive thrombus and venous stenosis when compared with 2-D TOF MRV [51].

Conclusion

The radiologist plays an important role in the early detection of pediatric cerebral sinovenous thrombosis. Advancements in medical imaging technology, particularly US, CT and MRI, have facilitated more accurate and timely diagnosis. However, despite an array of advanced imaging tools and techniques, the diagnosis of CSVT is often elusive. Given that the referring physician might not even suspect the diagnosis of CSVT and that the patient's symptoms and signs are often non-specific, the radiologist's responsibility is heightened to detect subtle imaging clues that suggest the presence of cerebral sinovenous thrombosis.

An understanding of the normal neonatal and young infant brain attenuation and the appearance of normal venous structures on unenhanced CT goes a long way in avoiding false-positive interpretations of venous thrombosis. If suspicion arises over CSVT upon CT review, the use of Hounsfield unit measurements and H:H ratios might improve diagnostic accuracy, although this has not been validated in the pediatric population. Routine coronal and sagittal reformations from axial helical unenhanced CT help to distinguish dural venous thrombosis from subdural drop

Table 3 Parameters used for enhanced MRV

Series: Sagittal SPGR 3-D MRV
Parameters:
• FOV 24.0
• Slice thickness 2.0 mm
• Matrix 256/192 (frequency/phase)
• NEX 1.0
• ASSET acceleration factor 1.0
• TE in-phase TI 300
• Receiver bandwidth 31.25
Contrast agent:
• Gadobutrol (Gadovist, Bayer HealthCare, Wayne, NJ)
• Dosage 1 mmol/kg or 0.1 ml/kg
• Injection rate: hand injection (0.5–2 ml/s)
• Flush with 5–15 ml 0.9% NaCl

A Signa HDxt (GE Healthcare, Milwaukee, WI) MRI scanner was used

SPGR spoiled gradient echo, *MRV* MR venography, *FOV* field of view, *NEX* number of excitations, *ASSET* array spatial sensitivity encoding technique

adjacent and epidural hemorrhage. A quick move to CT venography in questionable cases can clinch the diagnosis of CSVT. However, be aware that in normal newborns and young infants, the normal enhancing inner dura on enhanced CT and CT venography examinations can mimic venous sinus thrombosis. Therefore, if pandural venous sinus clot is suggested on the CT venography or the clinical presentation is incongruous with the CT venography results, supplement with high-resolution cranial sonography with color and pulsed Doppler to either verify or dismiss the diagnosis of CSVT. Routine review of the 2-D GRE MRI scout imaging and lateral extension of unenhanced sagittal T1-weighted imaging along with routine inclusion of coronal GRE imaging and a low threshold for performing contrast-enhanced 3-D SPGR MRV with multiplanar isotropic reconstructions all aid the radiologist in making a more timely and accurate diagnosis of cerebral sinovenous thrombosis.

Acknowledgments I would like to thank Ms. Starlyn Brandt for manuscript preparation and acknowledge the following colleagues for referring cases for this review: Drs. Richard Boyer, Kevin Moore, John Rampton, Dave Dansie and Logan Mclean.

References

1. Leach JL, Fortuna RB, Jones BV et al (2006) Imaging of cerebral venous thrombosis: current techniques, spectrum of findings, and diagnostic pitfalls. Radiographics 26:S19–S41, discussion S42-S43
2. Jonas Kimchi T, Lee SK, Agid R et al (2007) Cerebral sinovenous thrombosis in children. Neuroimaging Clin N Am 17:239–244
3. Carvalho KS, Bodensteiner JB, Connolly PJ et al (2001) Cerebral venous thrombosis in children. J Child Neurol 16:L574–L580
4. Shroff M, deVeber G (2003) Sinovenous thrombosis in children. Neuroimaging Clin N Am 13:115–138
5. Shevell MI, Silver K, O'Gorman AM et al (1989) Neonatal dural sinus thrombosis. Pediatr Neurol 5:161–165
6. Huisman TA, Holzmann D, Martin E et al (2001) Cerebral venous thrombosis in childhood. Eur Radiol 11:1760–1765
7. Wasay M, Dai AI, Ansari M et al (2008) Cerebral venous sinus thrombosis in children: a multicenter cohort from the United States. J Child Neurol 23:26–31
8. Tan M, deVeber G, Shroff M et al (2011) Sagittal sinus compression is associated with neonatal cerebral sinovenous thrombosis. Pediatrics 128:e429–e435
9. Sebire G, Tabarki B, Saunders DE et al (2005) Cerebral venous sinus thrombosis in children: risk factors, presentation, diagnosis and outcome. Brain 128:477–489
10. DeVeber G, Andrew M, Adams C et al (2001) Cerebral sinovenous thrombosis in children. N Engl J Med 345:417–423
11. Raybaud C (2010) Normal and abnormal embryology and development of the intracranial vascular system. Neurosurg Clin N Am 21:399–426
12. Jimenez JL, Lasjuanias P, Terbrugge K et al (1989) The transcerebral veins: normal and non-pathologic angiographic aspects. Surg Radiol Anat 11:63–72
13. Oran I, Memis A, Sener RN et al (1999) The so-called transcerebral veins: appearance in three different cases. Comput Med Imag Graph 23:127–131
14. Benedict SL, Bonkowsky JL, Thompson JA et al (2004) Cerebral sinovenous thrombosis in children: another reason to treat iron deficiency anemia. J Child Neurol 19:526–531
15. Krasnokutsky M (2011) Cerebral venous thrombosis: a potential mimic of primary traumatic brain injury in infants. AJR 197: W503–W507
16. Barnes PD (2011) Imaging of nonaccidental injury and the mimics: issues and controversies in the era of evidence-based medicine. Radiol Clin North Am 49:205–209
17. Barnes PD, Krasnokutsky M (2007) Imaging of the central nervous system in suspected or alleged nonaccidental injury, including the mimics. Top Magn Reson Imag 18:53–74
18. Singh S, Kumar S, Joseph M et al (2005) Cerebral venous sinus thrombosis presenting as subdural haematoma. Australas Radiol 49:101–103
19. Matsuda M, Matsuda I, Sato M et al (1982) Superior sagittal sinus thrombosis followed by subdural hematoma. Surg Neurol 18:206–211
20. Takamura Y, Morimoto S, Uede T et al (1996) Cerebral venous sinus thrombosis associated with systemic multiple hemangiomas as chronic subdural hematoma—case report. Neurol Med Chir (Tokyo) 36:650–653
21. Kalita J, Bansal V, Misra UK et al (2008) Intracerebral hemorrhage due to cerebral venous sinus thrombosis. QJM 101:247–249
22. McLean LA, Frasier LD, Hedlund GL (2012) Does intracranial venous thrombosis cause subdural hemorrhage in the pediatric population? AJNR. doi:10.3174/ajnr.A2967, Epub ahead of print
23. Tang PH, Chai J, Chan YH et al (2008) Superior sagittal sinus thrombosis: subtle signs on neuroimaging. Ann Acad Med Singapore 37:397–401
24. Zimmerman RD, Ernst RJ (1992) Neuroimaging of cerebral venous thrombosis. Neuroimage Clin North Am 2:463–485
25. Provenzale J, Kranz P (2011) Dural sinus thrombosis: sources of error in image interpretation. AJR 196:23–31
26. Provenzale JM, Joseph G, Barboriak D (1998) Dural sinus thrombosis: findings on CT and MR imaging and diagnostic pitfalls. AJR 170:777–783
27. Linn J, Pfefferkorn T, Ivanicova K et al (2009) Noncontrast CT in deep cerebral venous thrombosis and sinus thrombosis: comparison of its diagnostic value for both entities. AJNR 30:728–735
28. Virapongse C, Cazenave C, Quisling R et al (1987) The empty delta sign: frequency and significance in 76 cases of dural sinus thrombosis. Radiology 162:779–785
29. Nelson MD, Thompson JR, Hinshaw DB et al (1981) Radiodense dural sinuses: new CT sign in patients at risk for hypoxemic insult. AJNR 2:545–548
30. Ferro JM, Canhao P, Stam J et al (2009) Delay in the diagnosis of cerebral vein and dural sinus thrombosis: influence on outcome. Stroke 40:3133–3138
31. Majoie CB, van Straten M, Venema HW et al (2004) Multisection CT venography of the dural sinuses and cerebral veins by using mask bone elimination. AJNR 24:787–791
32. Black DF, Rad AE, Gray LA et al (2011) Cerebral venous sinus density on noncontrast CT correlates with hematocrit. AJNR 32:1354–1357
33. Puig J, Pedraza S, Demchuk A et al (2012) Quantification of thrombus Hounsfield units on noncontrast CT predicts stroke subtype and early recanalization after intravenous recombinant tissue plasminogen activator. AJNR 33:90–96
34. Croft P, Reichard R (2009) Microscopic examination of grossly unremarkable pediatric dura mater. Am J Forensic Med Pathol 30:10–13
35. Valdueza JM, Schultz M, Harms L et al (1995) Venous transcranial Doppler ultrasound monitoring in acute dural sinus thrombosis. Report of two cases. Stroke 26:1196–1199

36. Tsai FY, Wang AM, Matovich VB et al (1995) Acute thrombosis of the intracranial dural sinus; direct thrombolytic treatment. AJNR 16:2021–2029
37. Sze G, Simmons B, Krol G et al (1988) Dural sinus thrombosis: verification with spin-echo techniques. AJNR 9:679–686
38. Selim M, Fink J, Linfante I et al (2002) Diagnosis of cerebral venous thrombosis with echo-planar T2*-weighted magnetic resonance imaging. Arch Neurol 59:1021–1026
39. Tsuruda JS, Shimakawa A, Pelc NJ et al (1991) Dural sinus occlusion: evaluation with phase-sensitive gradient-echo MR imaging. AJNR 12:481–488
40. Thamburaj K, Choudhary A (2009) Hyperintense vessel sign: isolated cortical venous thrombosis after L-asparaginase therapy. Pediatr Radiol 39:757
41. Leach JL, Bluas RV, Ernst RJ et al (1996) MR imaging of isolated cortical vein thrombosis: the hyperintense vein sign. J Neurovasc Dis 1:1–7
42. Baumgartner RW, Studer A, Arnold M et al (2003) Recanalisation of cerebral venous thrombosis. J Neurol Neurosurg Psychiatry 74:459–461
43. Idbaih A, Boukobza M, Crassard I et al (2006) MRI clot in cerebral venous thrombosis. High diagnostic value of susceptibility-weighted images. Stroke 37:991–995
44. Ducreux D, Oppenheim C, Vandamme X et al (2001) Diffusion-weighted imaging patterns of brain damage associated with cerebral venous thrombosis. AJNR 22:261–268
45. Favrole P, Guichard J, Crassard I et al (2004) Diffusion-weighted imaging of intravascular clots in cerebral venous thrombosis. Stroke 35:99–103
46. Yoshikawa T, Abe O, Tsuchiya K et al (2002) Diffusion-weighted magnetic resonance imaging of dural sinus thrombosis. Neuroradiology 44:481–488
47. Widjaja E, Shroff M, Blaser S et al (2006) 2D time-of-flight MR venography in neonates: anatomy and pitfalls. AJNR 27:1913–1918
48. Widjaja E, Griffiths PD (2004) Intracranial MR venography in children: normal anatomy and variations. AJNR 25:1557–1562
49. Ayanzen RH, Bird CR, Keller PJ et al (2000) Cerebral MR venography: normal anatomy and potential diagnostic pitfalls. AJNR 21:74–78
50. Leach JL, Jones BV, Tomsick TA et al (1996) Normal appearance of arachnoid granulations on contrast-enhanced CT and MR of the brain: differentiation from dural sinus disease. AJNR 17:1523–1532
51. Klingebiel R, Bauknecht HC, Bohner G et al (2007) Comparative evaluation of 2D time-of-flight and 3D elliptic centric contrast-enhanced MR venography in patients with presumptive cerebral venous and sinus thrombosis. Eur J Neurol 14:139–143